Mineralogical Magazine, April 2002, Vol. 66(2), pp. 261–274

Optical properties and crystal structure of triclinic growth sectors in vesuvianite

T. TANAKA*, M. AKIZUKI AND Y. KUDOH

Institute of Mineralogy, Petrology and Economic Geology, Faculty of Science, Tohoku University, Aoba-ku, Sendai 980-8578, Japan

ABSTRACT

Sectored vesuvianite showing optically triclinic properties was studied by X-ray and P-FTIR analyses, and the origins of the internal optical texture are discussed. A monoclinic refinement (space group $P2/n$) suggests that site occupancies are slightly different among the Al(2) series, though the OH^- dipole is randomly oriented in all sectors. A relationship between the surface and internal texture suggests that these sectoral structures were produced during crystal growth, not by phase transitions.

KEYWORDS: crystal structure, growth sectors, vesuvianite, crystal growth.

Introduction

VESUVIANITE ($Ca_{19}(Mg,Fe^{2+},Al,Fe^{3+})_{13}Si_{18}O_{68}(O,OH,F)_{10}$) is a widely-occurring rock-forming mineral (e.g. Johnson *et al.*, 2000; Matsubara *et al.*, 1998), but there remain certain problems related to its crystal structure, optical properties and chemical composition.

The space group of vesuvianite was first pronounced as $P4/nnc$ by Warren and Modell (1931), and this has been thought to be fundamental in the symmetry of vesuvianite (e.g. Lager *et al.*, 1999). The crystal structure, however, has since been refined to space group $P4nc$ or $P4/n$ (e.g. Fitzgerald *et al.*, 1986, 1987; Ohkawa *et al.*, 1994; Armbruster and Gnos, 2000). Some vesuvianite crystals show weak reflections violating extinction rules on the <110> glide plane. Groat *et al.* (1993) observed X-ray precession photographs parallel to the b^*-c^* and a^*-b^* planes, and found violating reflections suggesting $P4/n$ in some specimens with sectoral texture. Veblen and Wiechmann (1991) examined selected-area electron diffraction (SAED) patterns on 110* and found numerous strong diffraction spots with $k + l = 2n + 1$, which are consistent with violation of the {100} n-glide extinction rules in space group $P4/nnc$. They suggested that the violating diffractions are caused by the fine-scale domains, and that the space group is $P2/n$ or lower. Some vesuvianite crystals are optically biaxial, and therefore their structure must have lower than tetragonal symmetry.

Optical symmetry is lower than morphological symmetry in some minerals, and this phenomenon has been referred to as 'optical anomaly' since the 19th century (Mallard, 1877). It has been suggested that the origin of these anomalies in many cases is crystal strain (e.g. Brauns, 1883). Although the morphological symmetry of vesuvianite is tetragonal, its optical anomaly has been known since the 19th century (e.g. Brauns, 1891). The origin was explained as a strain or impurity in the crystal structure. Recently, the origin of the optical anomaly of vesuvianite was explained as psuedomerohedral twins of fine-scale domains resulting from a phase transition between a high-temperature $P4/nnc$ and a low-temperature $P2/n$ or lower structure (Veblen and Wiechmann, 1991). Groat *et al.* (1993) suggested that the origin of low symmetry is due to the ferroelastic phase transition, in which the space group is reduced from $P4/nnc$ to $P4/n$. On the other hand, Allen and Burnham (1992) suggested that the origin of the low optical symmetry is due to cation ordering during crystal

* E-mail: t-tanaka@mail.cc.tohoku.ac.jp
DOI: 10.1180/0026461026620027

growth. Thus, the origin of the optical anomaly of vesuvianite is not, as yet, definite.

The purpose of the present study is to analyse the crystal structure of optically triclinic vesuvianite, and discuss the origin of low-symmetry sectors.

Experimental

Optical observation

The specimens studied are from Bellecombe, Aosta, Italy. The crystal form observed by the scanning electron microscope is shown in Fig. 1. The crystal size is small (~1 × 1 × 5 mm) and the crystal habit is variable. The colour is dark brown. The thin-sections parallel to the (001) and (110) faces are shown in Figs 2 and 4, respectively. This specimen is not altered, and the texture is clear under an optical microscope with crossed nicols. The specimens show optical growth sectors corresponding to the crystal faces. Some specimens from the same locality, however, are homogeneous when viewed between crossed nicols. Figure 3 shows a schematic sketch of Fig. 2. Detailed optical observation suggests that the optical indicatrix axes are not parallel to the morphological crystallographic axes in either the {110} or the {111} sectors. In addition, the {110} and {111} sectors have several twins parallel to the (110) face, suggesting that the sectors are monoclinic or triclinic. In Fig. 4, the two black and white sectors related by twins correspond with the {111} sector. The optic indicatrix axis, X, inclines at 3° to the c axis, and therefore all optic indicatrix axes of the {111} sector are not parallel to the crystallographic axes, indicating optically triclinic symmetry. Furthermore, the 2V value is larger in the {111} sector ($2V\alpha = 45°$) than in the {110} sector ($2V\alpha = 25°$), suggesting that the triclinicity of the {111} sector is greater than that of the {110} sector.

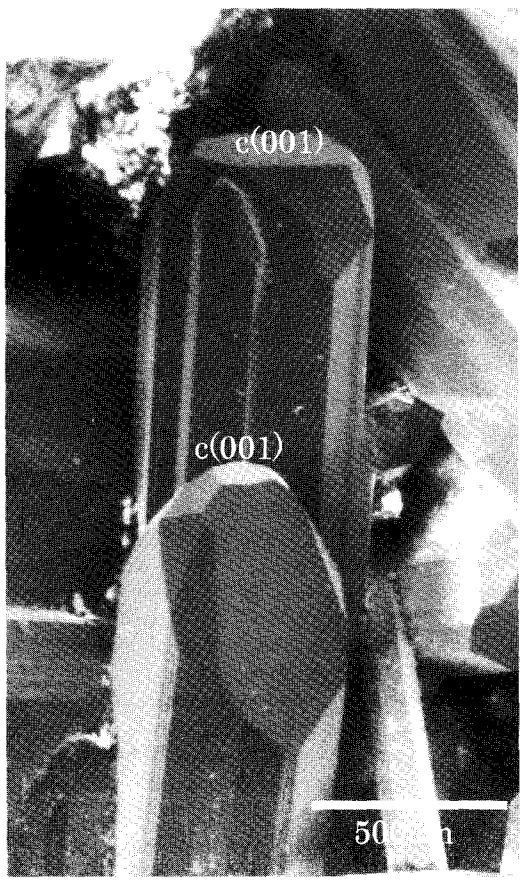

FIG. 1. SEM micrograph of vesuvianite from Bellecombe, Aosta, Italy. The (001) face is small in the nearer crystal, but larger in that to the rear.

Chemical composition

The chemical composition was analysed by electron microprobe analysis (JEOL-8800M) (Table 1), showing no significant difference between the sectors. According to Groat *et al.* (1992), B-bearing vesuvianite is optically positive, and vesuvianite without B is negative. The present specimens are optically negative, and therefore B is assumed to be low in these specimens, though it was not analysed.

Thermal and P-FTIR studies

Although the specimens were heated up to 800 °C, the sectors were still observed between crossed nicols, after cooling back to room temperature. The 2V value of the sectors, however, became smaller after heating than before.

The triclinic sectors of the unheated specimens were observed by polarized Fourier Transform Infrared Spectroscopy (P-FTIR) (JEOL JIR-DIAMOND-20 FTIR microspectrometer) in order to obtain the OH-vibration spectra. The observation shows that the OH dipole is not in any preferred orientation in this specimen.

Crystal structure refinement

The single crystals were handpicked from the {110} and {111} sectors in the section parallel to

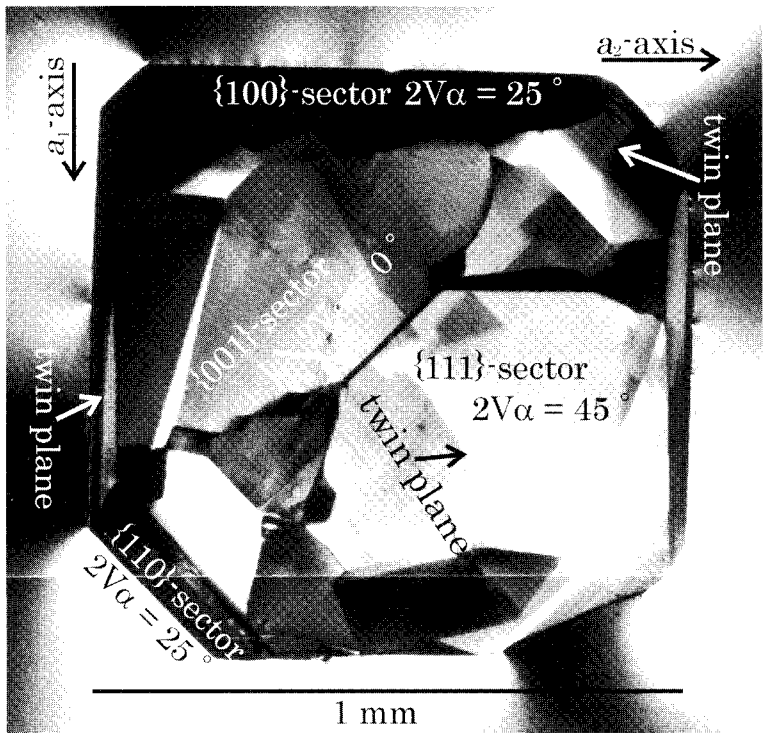

FIG. 2. The {001}, {110}, {111} and other sectors with high index in the thin-section parallel to the (001) face. The {001} sector is uniaxial, whereas the other sectors are biaxial ($2V\alpha = 25^\circ$ in the {110} sector, $2V\alpha = 45^\circ$ in the {111} sector). Crossed nicols.

(001) face. The {100} sector is small, and therefore the crystal could not be handpicked from this sector. The specimen of the {110} sector used for the study is $70 \times 60 \times 60$ μm and the {111} sector is $80 \times 70 \times 70$ μm in size. The lattice parameters were measured with a kappa four-circle diffractometer (MAC Science, MXC) with graphite-monochromated Mo-$K\alpha$ radiation (λ = 0.71073 Å) by a least-squares procedure applied to sin 2θ values of 48 reflections ranging from 30 to 35° (Table 2). The precession photographs ($\mu = 30^\circ$, 72 h exposure) parallel to the a^*-b^*, b^*-c^*, and 110* planes show no streaks or symmetry violating diffractions. In the lattice parameters of the {110} and {111} sectors, the β angle is slightly larger than 90°, and the α, γ angles are ~90°, indicating monoclinic symmetry.

The optic orientation shows that both the {110} and {111} sectors are triclinic, whereas the lattice parameters indicate monoclinic symmetry in these sectors. Since the triclinicity is low, the crystal structure refinements were carried out in monoclinic symmetry.

The linear absorption coefficient is ~30.6/cm, and therefore the difference of transmission factor between long and short lengths is ~3%, and can be ignored.

X-ray diffraction intensity data were measured at room temperature using the ω-2θ scan method from 3 to 60° in the {110} sector and from 3 to 55° in the {111} sector on an automated four-circle single-crystal X-ray diffractometer with graphite-monochromated Mo-$K\alpha_1$ radiation (λ = 0.70930 Å). Scattering factors for all atoms were taken from the International Tables for X-ray Crystallography (1974). After Lorentz and polarization corrections, sets of intensity data were obtained. No absorption corrections were made because of the small difference in transmission factor.

Since a Wilson plot showed the existence of an inversion centre in the structure, the space group

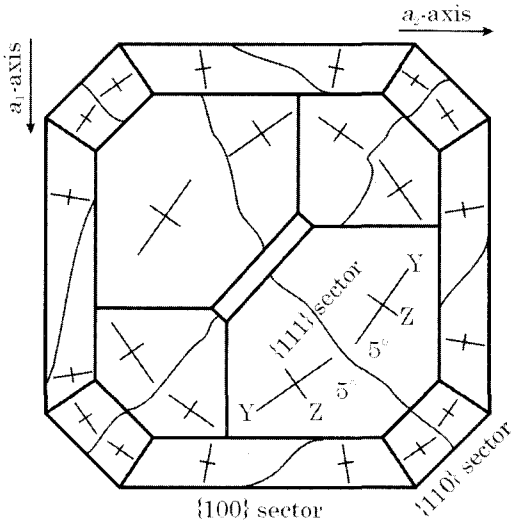

FIG. 3. Schematic internal texture in the (001) thin-section shown in Fig. 2. The *Z* axis is nearly parallel to the morphological [100] direction in the {100} sector, though that is nearly parallel to the morphological [110] direction in the {110} and {111} sectors. The angles between the Z axis and morphological [110] direction are 5° in the {111} and {110} sectors and between the *Z* axis and the [100] direction, 5° in the {100} sectors also. Some curved lines show composition planes of twinning.

must correspond to *P*2/*n*, not *Pn*. Therefore the crystal structures were refined using a full-matrix least-squares method in monoclinic *P*2/*n*.

The starting atomic coordinates for the monoclinic refinements were derived from the tetragonal structure given by Lager *et al.* (1999). All calculations were performed using the teXsan crystallographic software package of the Molecular Structure Corporation (1985, 1992). The results of the refinement are given in Table 3.

The atomic coordinates and anisotropic displacement parameters are listed in Tables 4*a*, 4*b*, 5*a* and 5*b*. Selected interatomic distances are summarized in Tables 6*a* and 6*b*. There are slight differences between Al(2a)–O(2a) and Al(2b)–O(2b) and between Al(2a)–O(11a) and Al(2b)–O(11b) in the {110} sector, and between Al(2b)–O(2b) and Al(2d)–O(2d) in the {111} sector. Thus, both sectors are monoclinic.

The site occupancies of Al in the four Al(1) sites and the four Al(2) sites are shown in Table 7. Although the site occupancies of Al are similar among the four Al(1) sites in both the {110} and {111} sectors, the slight difference is observed at the four Al(2) sites. The differences in site occupancies of the Al(2) series are larger in the {111} sector than in the {110} sector.

TABLE 1. Chemical analyses determined by EPMA.

	{100}, {110} sector	{001}, {111} sector
SiO_2	37.13	37.35
TiO_2	1.09	1.21
Al_2O_3	13.77	13.79
Fe_2O_3	6.51	6.29
MnO	0.16	0.15
MgO	2.82	2.84
CaO	36.49	36.49
Na_2O	0.00	0.00
K_2O	0.00	0.00
Si	18.00	18.00
Ti	0.40	0.44
Al	7.87	7.83
Fe^{3+}	2.38	2.28
Mn	0.07	0.06
Mg	2.04	2.04
Ca	18.95	18.84
Na	0.00	0.00
K	0.00	0.00

Vesuvianite formula calculated on the basis of 18 Si

TABLE 2. Lattice parameters of {110} and {111} sectors in vesuvianite.

{110} sector						
a	*b*	*c*	α	β	γ	V_{unit}
15.581(2)	15.591(2)	11.857(2)	90.00(1)	90.05(1)	90.01(1)	2880.31(60)
{111} sector						
a	*b*	*c*	α	β	γ	V_{unit}
15.582(2)	15.586(2)	11.855(1)	89.99(1)	90.05(1)	89.99(1)	2879.04(54)

Using 48 reflections in the range $30.0 < 2\theta < 35.0°$

TABLE 3. Mode of data collection of vesuvianite.

Sector	{110} sector	{111} sector
Dimension of crystal (mm^3)	$0.07 \times 0.06 \times 0.06$	$0.08 \times 0.07 \times 0.07$
Refinement space group	*P2/n*	*P2/n*
Scan type	ω-2θ	ω-2θ
Max. 2θ	60.0	55.0
Reflections measured	17312	7209
Unique reflection	9355	7020
Reflections used in the refinement ($I > 3\sigma_I$)	5705	4602
R value (%)	6.9	6.8
Rw value (%)*	5.0	5.6
GoF	1.42	1.85

* $w = 1/\sigma^2$

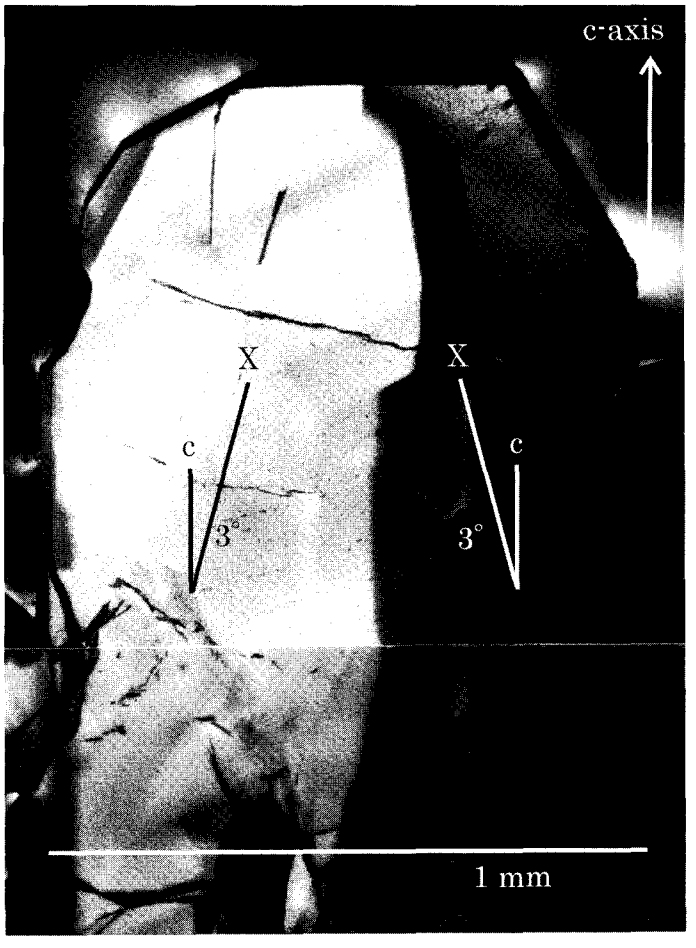

FIG. 4. Polarized photograph showing the {111} growth sector in a section parallel to (110). The optic indicatrix axis *X* inclines symmetrically at 3° to the *c* axis in the two black and white sectors, which are related by twinning. Crossed nicols.

Discussion

Optical observation and crystal structure

The specimen is optically biaxial, and the symmetry is triclinic, though the triclinicity is low. Tetragonal vesuvianite shows two kinds of diads: one is parallel to [100] and the other is parallel to [110]. Figure 3 shows that the optical indicatrix axis Z is approximately parallel to the [100] direction in the {100} sector, and is approximately parallel to the [110] direction in the both {110} and {111} sectors. The monoclinic diad obtained by XRD corresponds to the Z direction, i.e. the crystal orientations are different in different sectors.

Since the first crystal structure analysis of Warren and Modell (1931), several different models have been proposed for the structure of vesuvianite. Although the space group was assumed to be *P*4/*nnc* by Warren and Modell (1931), Armbruster and Gnos (2000) refined the crystal structure to space groups *P*4*nc* and *P*4/*n*. The 4- and $\bar{4}$-fold axes, however, were not observed in the present specimens. Since the specimen is optically triclinic, the correct structural symmetry must be triclinic, even if the triclinicity is low.

The differences of Al occupancy between Al(2a) and Al(2b), and Al(2c) and Al(2d) are 5.8 and 4.4 times standard deviation in the {110} sector, respectively. Also, the difference is 9.0 and 5.3 times in the {111} sector, respectively. Therefore the symmetry is reduced from tetragonal to at least monoclinic in both the {110} and {111} sectors. Furthermore, the difference in the Al occupancy in the {111} sector ($2V\alpha = 45°$) is larger than that in the {110} sector ($2V\alpha = 25°$) (Fig. 5). It is suggested that the triclinicity is greater in the {111} sector than in the {110} sector. X-ray analysis correlates with the optical observation.

Origin of sectoral structure

Similar sectors are observed in adularia (Akizuki and Sunagawa, 1978), topaz (Akizuki *et al.*, 1979), grossular-andradite garnet (Akizuki, 1984; Shtukenberg *et al.*, 2001), apophyllite (Akizuki and Terada, 1998) and some other minerals (e.g. alum in Shtukenberg *et al.*, 2000). It is thought that the sectors result from cation (Al^{3+}/Si^{4+}, Al^{3+}/Fe^{3+}) or anion (OH^-/F^-) ordering or preferred orientation of the OH^- dipole during crystal growth.

Akizuki *et al.* (1979) suggested that the sectoral textures of topaz become extinct upon heating, and Akizuki and Terada (1998) suggested that the low symmetry of apophyllite is due to preferred orientation of the OH^- dipole. Groat *et al.* (1993) found that the sectors of vesuvianite are extinct at 500°C, and Groat *et al.* (1995) suggested the substitution of H and B atoms, after interpretation of the IR spectra in the OH region of tetragonal

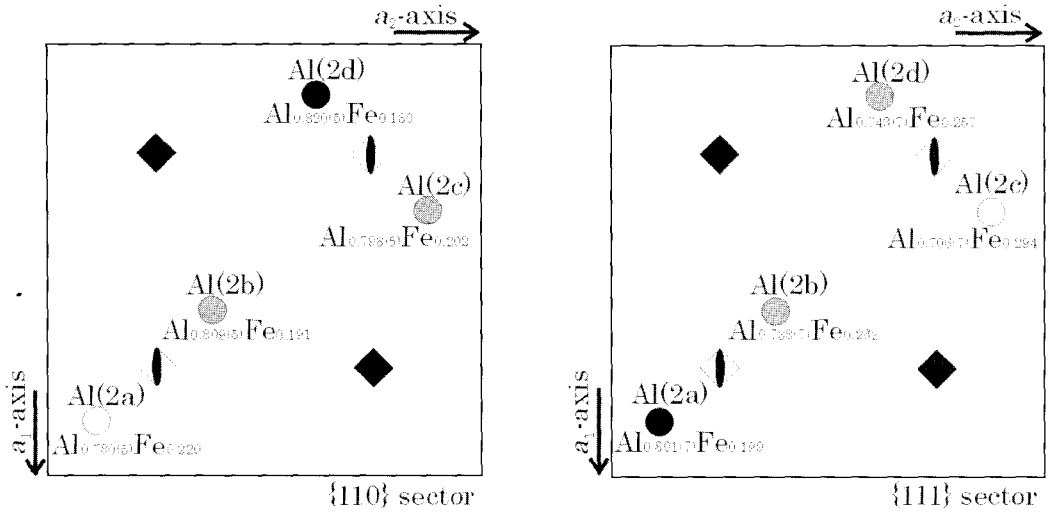

FIG. 5. Al site occupancies of Al(2) series around the $\bar{4}$-fold axis in {110} and {111} sectors. The difference of Al population in the {111} sector is larger than that in the {110} sector.

TABLE 4*a*. Atomic coordinates of {110} sector in vesuvianite.

Atom	*x*	*y*	*z*	B_{eq}(Å^2)	Atom	*x*	*y*	*z*	B_{eq}(Å^2)
Ca	−0.2498(2)	−0.2499(2)	0.1493(2)	0.53(4)	O(2b)	0.6172(3)	0.3392(3)	0.2805(4)	0.46(8)
Ca(1a)	−0.2500	0.2502(1)	0.2500	0.39(3)	O(2c)	0.3393(3)	−0.1174(3)	0.2794(4)	0.43(8)
Ca(1b)	0.2500	−0.2500(1)	0.2500	0.40(3)	O(2d)	0.1604(3)	0.6170(3)	0.2800(4)	0.42(8)
Ca(2a)	−0.18914(8)	0.04437(9)	0.3797(1)	0.41(2)	O(3a)	−0.0473(3)	0.2227(3)	0.0734(4)	0.49(8)
Ca(2b)	0.68921(8)	0.45565(9)	0.3796(1)	0.36(2)	O(3b)	0.5471(3)	0.2769(3)	0.0733(4)	0.35(8)
Ca(2c)	0.45594(9)	−0.18920(8)	0.3794(1)	0.40(2)	O(3c)	0.2772(3)	−0.0473(3)	0.0741(4)	0.48(8)
Ca(2d)	0.04416(9)	0.68911(8)	0.3799(1)	0.40(2)	O(3d)	0.2228(3)	0.5474(3)	0.0739(4)	0.41(8)
Ca(3a)	−0.10136(9)	−0.18173(10)	0.8882(1)	1.13(3)	O(4a)	−0.0612(3)	0.1055(3)	0.4701(4)	0.51(8)
Ca(3b)	0.60113(9)	0.68176(9)	0.8878(1)	0.99(3)	O(4b)	0.5606(3)	0.3942(3)	0.4707(4)	0.49(8)
Ca(3c)	0.68183(9)	−0.10125(9)	0.8880(1)	1.03(3)	O(4c)	0.3938(3)	−0.0609(3)	0.4694(4)	0.50(8)
Ca(3d)	−0.18165(9)	0.60127(9)	0.8882(1)	1.10(3)	O(4d)	0.1065(3)	0.5615(3)	0.4693(4)	0.46(8)
Si(1)	−0.2499(1)	0.2500(1)	0.0000(1)	0.29(3)	O(5a)	−0.1705(3)	0.0133(3)	0.1802(4)	0.61(9)
Si(2a)	−0.1803(1)	0.0402(1)	0.8717(1)	0.29(3)	O(5b)	0.6711(3)	0.4865(3)	0.1804(4)	0.59(9)
Si(2b)	0.6805(1)	0.4600(1)	0.8714(1)	0.31(3)	O(5c)	0.4867(3)	−0.1710(3)	0.1803(4)	0.56(8)
Si(2c)	0.4596(1)	−0.1805(1)	0.8715(1)	0.26(3)	O(5d)	0.0135(3)	0.6700(3)	0.1797(4)	0.70(9)
Si(2d)	0.0402(1)	0.6803(1)	0.8714(1)	0.24(3)	O(6a)	−0.1203(3)	−0.2722(3)	0.0588(4)	0.76(9)
Si(3a)	−0.0839(1)	−0.1506(1)	0.3641(1)	0.34(3)	O(6b)	0.6202(3)	0.7719(3)	0.0586(4)	0.91(9)
Si(3b)	0.5837(1)	0.6507(1)	0.3642(1)	0.34(3)	O(6c)	0.7722(3)	−0.1201(3)	0.0581(4)	0.84(9)
Si(3c)	0.6508(1)	−0.0838(1)	0.3641(1)	0.31(3)	O(6d)	−0.2719(3)	0.6206(3)	0.0588(4)	0.81(9)
Si(3d)	−0.1508(1)	0.5838(1)	0.3643(1)	0.36(3)	O(7a)	0.0556(3)	0.1730(3)	0.3202(4)	0.61(9)
Al(1a)	0.0000	0.0000	0.0000	0.40(5)	O(7b)	0.4443(3)	0.3273(3)	0.3204(4)	0.65(9)
Al(1b)	0.5000	0.5000	0.0000	0.44(5)	O(7c)	0.3270(3)	0.0554(3)	0.3207(4)	0.70(9)
Al(1c)	0.5000	0.0000	0.0000	0.46(5)	O(7d)	0.1727(3)	0.4445(3)	0.3203(4)	0.68(9)
Al(1d)	0.0000	0.5000	0.0000	0.51(5)	O(8a)	−0.0607(3)	−0.0914(3)	0.0660(4)	0.50(8)
Al(2a)	−0.1119(1)	0.1213(1)	0.1269(1)	0.42(4)	O(8b)	0.5611(3)	0.5909(3)	0.0654(4)	0.51(8)
Al(2b)	0.6118(1)	0.3785(1)	0.1270(1)	0.43(4)	O(8c)	0.5913(3)	−0.0612(3)	0.0665(4)	0.44(8)
Al(2c)	0.3787(1)	−0.1119(1)	0.1266(1)	0.47(4)	O(8d)	−0.0910(3)	0.5609(3)	0.0662(4)	0.52(8)
Al(2d)	0.1213(1)	0.6120(1)	0.1268(1)	0.32(4)	O(9a)	−0.1452(3)	−0.1452(3)	0.2501(4)	0.62(9)
Mg	−0.2497(1)	−0.2499(1)	0.0356(2)	0.78(4)	O(9b)	0.6451(3)	0.6459(3)	0.2499(4)	0.61(9)
O(1a)	−0.2207(3)	0.1728(3)	0.0838(4)	0.53(8)	O(10)	−0.2499(3)	−0.2497(4)	0.8650(5)	1.28(10)
O(1b)	0.7215(3)	0.3270(3)	0.0841(4)	0.46(8)	O(11a)	−0.0037(3)	0.0617(3)	0.1364(4)	0.70(9)
O(1c)	0.3270(3)	−0.2209(3)	0.0835(4)	0.52(8)	O(11b)	0.5025(3)	0.4390(3)	0.1362(4)	0.68(9)
O(1d)	0.1729(3)	0.7209(3)	0.0839(4)	0.45(8)	O(11c)	0.4386(3)	−0.0031(3)	0.1361(4)	0.56(8)
O(2a)	−0.1168(3)	0.1603(3)	0.2791(4)	0.51(8)	O(11d)	0.0615(3)	0.5032(3)	0.1362(4)	0.69(9)

Table 4*b*. Atomic coordinates of {111} sector in vesuvianite.

Atom	*x*	*y*	*z*	B_{eq}(Å^2)	Atom	*x*	*y*	*z*	B_{eq}(Å^2)
Ca	−0.2504(3)	−0.2493(3)	0.1472(4)	1.00(8)	Al(1b)	0.5000	0.5000	0.0000	0.38(9)
Ca(1a)	−0.2500	0.2496(2)	0.2500	0.44(5)	Al(1c)	0.5000	0.0000	0.0000	0.59(10)
Ca(1b)	0.2500	−0.2502(3)	0.2500	0.54(6)	Al(1d)	0.0000	0.5000	0.0000	0.41(9)
Ca(2a)	−0.1893(1)	0.0443(2)	0.3794(2)	0.50(4)	Al(2a)	−0.1119(2)	0.1215(2)	0.1272(2)	0.99(9)
Ca(2b)	0.6891(1)	0.4558(2)	0.3797(2)	0.45(4)	Al(2b)	0.6117(2)	0.3787(2)	0.1269(2)	0.98(10)
Ca(2c)	0.4554(1)	−0.1890(2)	0.3800(2)	0.44(4)	Al(2c)	0.3786(2)	−0.1115(2)	0.1270(2)	1.6(1)
Ca(2d)	0.0440(1)	0.6892(2)	0.3793(2)	0.46(4)	Al(2d)	0.1211(2)	0.6119(2)	0.1267(2)	1.2(1)
Ca(3a)	−0.1010(1)	−0.1816(2)	0.8882(2)	0.93(5)	Mg	−0.2502(2)	−0.2497(3)	0.0363(3)	1.30(9)
Ca(3b)	0.6012(2)	0.6819(2)	0.8879(2)	0.97(5)	O(1a)	−0.2221(5)	0.1725(5)	0.0853(6)	0.6(2)
Ca(3c)	0.6818(2)	−0.1011(2)	0.8882(2)	0.97(5)	O(1b)	0.7216(5)	0.3280(5)	0.0847(6)	0.3(1)
Ca(3d)	−0.1817(2)	0.6012(2)	0.8885(2)	0.98(5)	O(1c)	0.3278(5)	−0.2214(5)	0.0852(6)	0.5(1)
Si(1)	−0.2503(2)	0.2501(2)	0.0002(2)	0.25(5)	O(1d)	0.1731(5)	0.7218(5)	0.0840(6)	0.6(1)
Si(2a)	−0.1804(2)	0.0402(2)	0.8714(3)	0.41(6)	O(2a)	−0.1175(5)	0.1609(5)	0.2804(6)	0.7(2)
Si(2b)	0.6804(2)	0.4599(2)	0.8716(3)	0.29(6)	O(2b)	0.6169(1)	0.3399(5)	0.2787(6)	0.6(2)
Si(2c)	0.4595(2)	−0.1803(2)	0.8718(3)	0.34(6)	O(2c)	0.3386(5)	−0.1173(5)	0.2794(6)	0.6(2)
Si(2d)	0.0398(2)	0.6802(2)	0.8716(3)	0.40(6)	O(2d)	0.1606(5)	0.6171(5)	0.2807(6)	0.6(2)
Si(3a)	−0.0836(2)	0.1504(2)	0.3637(3)	0.39(6)	O(3a)	−0.0460(5)	0.2235(5)	0.0747(6)	0.5(1)
Si(3b)	0.5839(2)	0.6503(2)	0.3641(3)	0.46(6)	O(3b)	0.5473(5)	0.2773(5)	0.0745(6)	0.5(1)
Si(3c)	0.6505(2)	−0.0837(2)	0.3643(3)	0.47(6)	O(3c)	0.2771(5)	−0.0463(5)	0.0750(6)	0.6(2)
Si(3d)	−0.1502(2)	0.5839(2)	0.3648(3)	0.42(6)	O(3d)	0.2234(5)	0.5469(5)	0.0739(6)	0.6(2)
Al(1a)	0.0000	0.0000	0.0000	0.38(9)	O(4a)	−0.0615(4)	0.1061(5)	0.4692(6)	0.3(1)

Table 4*b*. (*contd.*) Atomic coordinates of {111} sector in vesuvianite.

Atom	*x*	*y*	*z*	B_{eq}(Å^2)	Atom	*x*	*y*	*z*	B_{eq}(Å^2)
O(4b)	0.5617(5)	0.3937(5)	0.4688(6)	0.6(2)	O(7c)	0.3272(5)	0.0560(5)	0.3232(7)	0.7(2)
O(4c)	0.3939(4)	−0.0612(5)	0.4694(6)	0.7(2)	O(7d)	0.1722(5)	0.4435(5)	0.3231(7)	0.7(2)
O(4d)	0.1062(5)	0.5610(5)	0.4693(6)	0.5(2)	O(8a)	−0.0612(5)	−0.0919(5)	0.0667(7)	0.6(2)
O(5a)	−0.1709(5)	0.0132(5)	0.1807(6)	0.7(2)	O(8b)	0.5613(5)	0.5911(5)	0.0667(7)	0.8(2)
O(5b)	0.6701(5)	0.4866(5)	0.1800(6)	0.7(2)	O(8c)	0.5923(5)	−0.0607(5)	0.0666(7)	0.7(2)
O(5c)	0.4866(5)	−0.1702(5)	0.1810(7)	0.8(2)	O(8d)	−0.0910(5)	0.5615(5)	0.0657(7)	0.8(2)
O(5d)	0.0127(5)	0.6714(5)	0.1793(6)	0.7(2)	O(9a)	−0.1450(5)	−0.1454(6)	0.2499(7)	0.9(2)
O(6a)	−0.1212(5)	−0.2728(5)	0.0600(6)	0.9(2)	O(9b)	0.6449(5)	0.6454(6)	0.2503(6)	0.9(2)
O(6b)	0.6203(5)	0.7724(5)	0.0592(6)	0.9(2)	O(10)	−0.2500(5)	−0.2495(7)	0.8617(7)	1.6(2)
O(6c)	0.7710(5)	−0.1209(5)	0.0595(6)	0.8(2)	O(11a)	−0.0033(5)	0.0613(5)	0.1352(7)	0.8(2)
O(6d)	−0.2727(5)	0.6206(5)	0.0601(7)	0.9(2)	O(11b)	0.5032(5)	0.4387(5)	0.1349(6)	0.7(2)
O(7a)	0.0554(5)	0.1731(5)	0.3233(6)	0.8(2)	O(11c)	0.4393(5)	−0.0037(5)	0.1334(6)	0.8(2)
O(7b)	0.4442(5)	0.3276(5)	0.3228(7)	0.9(2)	O(11d)	0.0612(5)	0.5035(5)	0.1346(6)	0.7(2)

TABLE 5*a*. Anisotropic displacement parameters of {110} sector.

Atom	U_{11}	U_{22}	U_{33}	U_{12}	U_{13}	U_{23}
Ca	0.004(1)	0.0010(10)	0.015(1)	−0.0005(9)	0.0014(9)	0.0001(10)
Ca(1a)	0.0099(8)	0.0030(7)	0.0021(7)	0.0000	−0.0008(6)	0.0000
Ca(1b)	0.0031(7)	0.0106(8)	0.0016(7)	0.0000	0.0005(6)	0.0000
Ca(2a)	0.0032(6)	0.0068(6)	0.0055(6)	0.0010(5)	−0.0002(4)	0.0010(4)
Ca(2b)	0.0039(6)	0.0045(6)	0.0053(6)	0.0009(4)	0.0013(4)	−0.0010(4)
Ca(2c)	0.0065(6)	0.0039(6)	0.0049(6)	−0.0005(4)	−0.0003(4)	−0.0002(4)
Ca(2d)	0.0055(6)	0.0040(6)	0.0056(6)	−0.0006(4)	0.0009(4)	0.0003(4)
Ca(3a)	0.0084(6)	0.0106(7)	0.0240(8)	0.0034(5)	−0.0078(6)	−0.0061(6)
Ca(3b)	0.0083(6)	0.0079(6)	0.0215(8)	0.0027(5)	0.0071(5)	0.0065(5)
Ca(3c)	0.0090(7)	0.0085(6)	0.0214(8)	−0.0037(5)	0.0078(5)	−0.0081(5)
Ca(3d)	0.0092(7)	0.0084(6)	0.0241(8)	−0.0037(5)	−0.0070(5)	0.0093(6)
Si(1)	0.0060(7)	0.0040(7)	0.0009(7)	−0.0003(6)	0.0008(5)	−0.0010(6)
Si(2a)	0.0029(8)	0.0042(8)	0.0037(8)	0.0003(6)	0.0006(6)	0.0014(6)
Si(2b)	0.0034(8)	0.0035(8)	0.0049(8)	−0.0004(6)	0.0003(6)	−0.0011(6)
Si(2c)	0.0031(8)	0.0029(7)	0.0039(8)	0.0007(6)	−0.0008(6)	−0.0004(6)
Si(2d)	0.0026(8)	0.0027(8)	0.0040(8)	−0.0002(6)	0.0016(6)	−0.0001(6)
Si(3a)	0.0081(8)	0.0016(7)	0.0031(8)	0.0006(6)	0.0001(6)	0.0004(6)
Si(3b)	0.0077(8)	0.0013(7)	0.0037(8)	0.0000(6)	0.0006(6)	0.0005(6)
Si(3c)	0.0013(7)	0.0065(8)	0.0040(8)	0.0002(6)	0.0000(6)	−0.0004(6)
Si(3d)	0.0005(7)	0.0077(8)	0.0052(8)	0.0006(6)	0.0005(6)	0.0000(6)
Al(1a)	0.002(1)	0.005(1)	0.007(1)	0.0013(10)	0.0008(10)	0.000(1)
Al(1b)	0.004(1)	0.007(1)	0.006(1)	0.002(1)	−0.0007(10)	0.002(1)
Al(1c)	0.005(1)	0.006(1)	0.006(1)	0.000(1)	0.001(1)	0.001(1)
Al(1d)	0.007(1)	0.005(1)	0.008(1)	−0.003(1)	0.001(1)	−0.001(1)
Al(2a)	0.006(1)	0.005(1)	0.006(1)	0.0002(9)	0.0029(8)	0.0010(9)
Al(2b)	0.005(1)	0.005(1)	0.006(1)	−0.0017(9)	−0.0018(8)	0.0006(8)
Al(2c)	0.004(1)	0.005(1)	0.009(1)	0.0000(9)	0.0000(8)	0.0011(9)
Al(2d)	0.004(1)	0.005(1)	0.003(1)	−0.0005(8)	0.0011(8)	−0.0016(8)
Mg	0.0030(10)	0.0033(10)	0.023(1)	0.0012(9)	0.0020(9)	−0.0028(10)
O(1a)	0.006(2)	0.006(2)	0.007(2)	−0.001(2)	0.000(2)	0.001(2)
O(1b)	0.009(2)	0.004(2)	0.005(2)	0.000(2)	0.001(2)	0.002(2)
O(1c)	0.006(2)	0.006(2)	0.008(2)	0.003(2)	0.003(2)	0.001(2)
O(1d)	0.007(2)	0.008(2)	0.002(2)	0.000(2)	−0.003(2)	0.001(2)
O(2a)	0.006(2)	0.004(2)	0.009(2)	−0.001(2)	−0.002(2)	0.001(2)
O(2b)	0.005(2)	0.008(2)	0.004(2)	−0.001(2)	0.000(2)	−0.001(2)
O(2c)	0.007(2)	0.006(2)	0.004(2)	0.002(2)	0.000(2)	−0.001(2)
O(2d)	0.005(2)	0.008(2)	0.003(2)	0.001(2)	0.000(2)	0.002(2)

TABLE 5*a*. (*contd.*) Anisotropic displacement parameters of {110} sector.

Atom	U_{11}	U_{22}	U_{33}	U_{12}	U_{13}	U_{23}
O(3a)	0.005(2)	0.004(2)	0.010(2)	−0.001(2)	−0.003(2)	−0.002(2)
O(3b)	0.004(2)	0.005(2)	0.004(2)	−0.002(2)	0.000(2)	0.001(2)
O(3c)	0.009(2)	0.004(2)	0.005(2)	0.001(2)	0.001(2)	−0.001(2)
O(3d)	0.006(2)	0.006(2)	0.003(2)	0.002(2)	0.000(2)	−0.001(2)
O(4a)	0.005(2)	0.007(2)	0.007(2)	0.000(2)	0.001(2)	−0.001(2)
O(4b)	0.006(2)	0.007(2)	0.005(2)	0.002(2)	0.000(2)	−0.001(2)
O(4c)	0.006(2)	0.009(2)	0.004(2)	0.000(2)	0.000(2)	−0.003(2)
O(4d)	0.006(2)	0.007(2)	0.005(2)	0.001(2)	0.001(2)	−0.002(2)
O(5a)	0.003(2)	0.013(2)	0.008(2)	0.004(2)	0.001(2)	−0.001(2)
O(5b)	0.005(2)	0.015(2)	0.003(2)	0.007(2)	0.000(2)	0.001(2)
O(5c)	0.011(2)	0.005(2)	0.004(2)	−0.005(2)	0.001(2)	0.000(2)
O(5d)	0.012(2)	0.008(2)	0.006(2)	−0.003(2)	0.002(2)	−0.002(2)
O(6a)	0.018(2)	0.007(2)	0.003(2)	0.002(2)	0.002(2)	0.002(2)
O(6b)	0.019(3)	0.009(2)	0.007(2)	0.002(2)	−0.002(2)	−0.002(2)
O(6c)	0.006(2)	0.019(3)	0.006(2)	−0.001(2)	−0.002(2)	0.002(2)
O(6d)	0.006(2)	0.018(3)	0.007(2)	−0.003(2)	0.003(2)	−0.005(2)
O(7a)	0.004(2)	0.008(2)	0.011(2)	0.000(2)	0.001(2)	−0.003(2)
O(7b)	0.008(2)	0.009(2)	0.008(2)	0.001(2)	−0.001(2)	0.001(2)
O(7c)	0.011(2)	0.010(2)	0.006(2)	−0.003(2)	0.002(2)	−0.002(2)
O(7d)	0.010(2)	0.006(2)	0.010(2)	−0.002(2)	−0.003(2)	0.000(2)
O(8a)	0.006(2)	0.005(2)	0.008(2)	−0.001(2)	0.002(2)	0.001(2)
O(8b)	0.003(2)	0.005(2)	0.011(2)	0.003(2)	−0.004(2)	−0.003(2)
O(8c)	0.004(2)	0.004(2)	0.009(2)	−0.004(2)	−0.002(2)	0.000(2)
O(8d)	0.004(2)	0.005(2)	0.011(2)	−0.001(2)	0.000(2)	−0.004(2)
O(9a)	0.012(2)	0.010(2)	0.002(2)	−0.001(2)	0.002(2)	0.001(2)
O(9b)	0.007(2)	0.009(2)	0.006(2)	−0.001(2)	0.000(2)	−0.001(2)
O(10)	0.009(2)	0.014(2)	0.026(3)	−0.001(2)	0.003(2)	0.001(2)
O(11a)	0.006(2)	0.006(2)	0.015(2)	−0.004(2)	0.000(2)	−0.002(2)
O(11b)	0.010(2)	0.008(2)	0.007(2)	−0.001(2)	0.002(2)	0.004(2)
O(11c)	0.007(2)	0.008(2)	0.006(2)	0.002(2)	0.003(2)	0.000(2)
O(11d)	0.009(2)	0.010(2)	0.008(2)	0.004(2)	−0.002(2)	0.000(2)

Table 5*b*. Anisotropic displacement parameters of {111} sector.

Atom	U_{11}	U_{22}	U_{33}	U_{12}	U_{13}	U_{23}
Ca	0.009(2)	0.007(2)	0.022(2)	0.000(2)	0.002(2)	0.000(2)
Ca(1a)	0.011(1)	0.003(1)	0.002(1)	0.0000	0.000(1)	0.0000
Ca(1b)	0.004(1)	0.015(2)	0.001(1)	0.0000	0.000(1)	0.0000
Ca(2a)	0.005(1)	0.007(1)	0.007(1)	−0.0001(9)	0.0003(8)	0.0020(9)
Ca(2b)	0.006(1)	0.005(1)	0.006(1)	−0.0001(9)	0.0004(8)	−0.0021(9)
Ca(2c)	0.006(1)	0.005(1)	0.005(1)	−0.0005(9)	−0.0013(8)	−0.0005(9)
Ca(2d)	0.007(1)	0.004(1)	0.007(1)	0.0004(9)	0.0013(8)	0.0006(9)
Ca(3a)	0.006(1)	0.010(1)	0.019(1)	0.0034(10)	−0.0076(9)	−0.006(1)
Ca(3b)	0.009(1)	0.009(1)	0.018(1)	0.0022(10)	0.0046(9)	0.005(1)
Ca(3c)	0.007(1)	0.009(1)	0.020(1)	−0.0025(10)	0.0064(10)	−0.007(1)
Ca(3d)	0.012(1)	0.007(1)	0.019(1)	−0.0028(10)	−0.0067(10)	0.0068(10)
Si(1)	0.003(1)	0.005(1)	0.001(1)	−0.001(1)	−0.0002(10)	0.000(1)
Si(2a)	0.004(1)	0.006(2)	0.005(1)	0.001(1)	0.001(1)	0.002(1)
Si(2b)	0.004(1)	0.004(1)	0.002(1)	−0.001(1)	−0.001(1)	−0.002(1)
Si(2c)	0.006(1)	0.004(1)	0.003(1)	−0.001(1)	−0.002(1)	0.000(1)
Si(2d)	0.004(1)	0.005(1)	0.006(1)	0.000(1)	−0.001(1)	0.000(1)
Si(3a)	0.009(1)	0.002(1)	0.004(1)	0.000(1)	0.000(1)	0.002(1)
Si(3b)	0.009(1)	0.003(1)	0.006(2)	−0.003(1)	−0.001(1)	−0.003(1)

Table 5*b*. (*contd.*) Anisotropic displacement parameters of {111} sector.

Atom	U_{11}	U_{22}	U_{33}	U_{12}	U_{13}	U_{23}
Si(3c)	0.003(1)	0.008(2)	0.006(2)	0.001(1)	−0.004(1)	0.002(1)
Si(3d)	0.002(1)	0.010(2)	0.004(1)	0.000(1)	0.003(1)	−0.001(1)
Al(1a)	0.003(2)	0.007(2)	0.003(2)	0.001(2)	−0.001(2)	0.000(2)
Al(1b)	0.002(2)	0.004(2)	0.007(2)	0.001(2)	0.002(2)	0.001(2)
Al(1c)	0.008(2)	0.003(2)	0.011(3)	−0.003(2)	0.002(2)	−0.001(2)
Al(1d)	0.004(2)	0.005(2)	0.007(2)	0.000(2)	0.000(2)	0.001(2)
Al(2a)	0.019(2)	0.010(2)	0.008(2)	−0.001(2)	0.003(2)	−0.002(2)
Al(2b)	0.009(2)	0.013(3)	0.014(3)	0.000(2)	−0.001(2)	0.000(2)
Al(2c)	0.024(3)	0.023(3)	0.013(3)	0.000(3)	0.002(2)	0.001(2)
Al(2d)	0.012(2)	0.017(3)	0.015(3)	0.002(2)	−0.001(2)	−0.006(2)
Mg	0.008(2)	0.008(2)	0.034(3)	0.002(2)	−0.001(2)	0.007(2)
O(1a)	0.014(4)	0.008(4)	0.001(4)	−0.003(3)	−0.002(3)	−0.002(3)
O(1b)	0.006(3)	0.006(4)	0.001(4)	0.000(3)	0.000(3)	0.001(3)
O(1c)	0.006(4)	0.008(4)	0.003(4)	−0.002(3)	0.000(3)	−0.002(3)
O(1d)	0.009(4)	0.013(4)	0.003(4)	0.003(3)	−0.004(3)	0.001(3)
O(2a)	0.009(4)	0.010(4)	0.006(4)	−0.006(3)	−0.006(3)	0.002(3)
O(2b)	0.006(3)	0.009(4)	0.007(4)	−0.003(3)	−0.001(3)	−0.001(3)
O(2c)	0.012(4)	0.006(4)	0.005(4)	0.003(3)	−0.001(3)	0.003(3)
O(2d)	0.013(4)	0.003(4)	0.005(4)	−0.001(3)	0.005(3)	−0.002(3)
O(3a)	0.006(4)	0.009(4)	0.005(4)	0.000(3)	0.004(3)	−0.001(3)
O(3b)	0.007(4)	0.008(4)	0.005(3)	0.000(3)	−0.003(3)	0.001(3)
O(3c)	0.012(4)	0.011(4)	0.001(4)	−0.002(3)	−0.001(3)	0.002(3)
O(3d)	0.009(4)	0.006(4)	0.009(4)	0.005(3)	−0.001(3)	−0.003(3)
O(4a)	0.006(4)	0.001(4)	0.005(4)	−0.001(3)	−0.002(3)	0.001(3)
O(4b)	0.004(4)	0.009(4)	0.010(4)	0.000(3)	0.002(3)	0.003(3)
O(4c)	0.002(3)	0.014(4)	0.011(4)	−0.001(3)	0.000(3)	0.000(3)
O(4d)	0.006(4)	0.007(4)	0.006(4)	−0.002(3)	−0.005(3)	0.001(3)
O(5a)	0.013(4)	0.007(4)	0.007(4)	0.003(3)	0.001(3)	−0.004(3)
O(5b)	0.012(4)	0.012(4)	0.004(4)	0.006(3)	0.002(3)	0.005(3)
O(5c)	0.010(4)	0.011(4)	0.011(4)	−0.004(3)	0.003(3)	−0.003(3)
O(5d)	0.009(4)	0.009(4)	0.008(4)	−0.007(3)	−0.003(3)	0.002(3)
O(6a)	0.018(4)	0.013(4)	0.002(3)	0.005(3)	0.000(3)	0.001(3)
O(6b)	0.020(4)	0.006(4)	0.009(4)	0.002(3)	−0.003(3)	−0.002(3)
O(6c)	0.012(4)	0.018(5)	0.002(4)	−0.003(4)	0.004(3)	−0.002(3)
O(6d)	0.009(4)	0.015(4)	0.011(4)	−0.003(3)	−0.002(3)	−0.001(4)
O(7a)	0.007(4)	0.017(5)	0.006(4)	−0.002(3)	0.000(3)	0.001(3)
O(7b)	0.011(4)	0.008(4)	0.014(4)	0.001(3)	0.001(3)	0.000(3)
O(7c)	0.012(4)	0.003(4)	0.012(4)	−0.001(3)	0.001(3)	−0.006(3)
O(7d)	0.003(4)	0.011(4)	0.012(4)	0.000(3)	−0.004(3)	0.001(3)
O(8a)	0.005(4)	0.006(4)	0.011(4)	0.000(3)	−0.002(3)	0.001(3)
O(8b)	0.006(4)	0.015(4)	0.009(4)	−0.003(3)	0.002(3)	0.003(3)
O(8c)	0.012(4)	0.002(4)	0.014(4)	0.000(3)	−0.002(3)	−0.004(3)
O(8d)	0.005(4)	0.010(4)	0.017(4)	−0.004(3)	−0.006(3)	0.006(3)
O(9a)	0.014(4)	0.014(5)	0.005(4)	−0.005(4)	0.005(3)	−0.005(3)
O(9b)	0.015(4)	0.016(5)	0.002(4)	−0.005(4)	0.000(3)	0.001(3)
O(10)	0.017(4)	0.023(5)	0.023(5)	0.007(4)	−0.002(4)	−0.002(5)
O(11a)	0.007(4)	0.011(4)	0.013(4)	−0.002(3)	−0.003(3)	−0.009(3)
O(11b)	0.013(4)	0.007(4)	0.007(4)	−0.002(3)	0.004(3)	0.005(3)
O(11c)	0.014(4)	0.007(4)	0.010(4)	0.000(3)	0.011(3)	−0.001(3)
O(11d)	0.009(4)	0.010(4)	0.008(4)	0.002(3)	−0.004(3)	0.000(3)

TABLE 6*a*. Selected interatomic distances (Å) of the {110} sector.

Ca-O(6a)	2.313(5)	Ca(2c)-O(5d)	2.353(5)	Ca(3d)-O(10)	2.570(7)	Al(2d)-O(5d)	2.010(5)
Ca-O(6b)	2.318(6)	Ca(2c)-O(6a)	2.961(5)	Ca(3d)-O(11d)	2.499(5)	Al(2d)-O(11d)	1.939(5)
Ca-O(6c)	2.320(6)	Ca(2c)-O(8a)	2.324(5)				
Ca-O(6d)	2.313(6)			Mg-O(6a)	2.065(5)	Si(1)-O(1a)	1.625(5)
Ca-O(9a)	2.597(6)	Ca(2d)-O(1c)	2.486(5)	Mg-O(6b)	2.074(5)	Si(1)-O(1b)	1.623(5)
Ca-O(9a)	2.601(5)	Ca(2d)-O(2d)	2.440(5)	Mg-O(6c)	2.070(6)	Si(1)-O(1c)	1.621(5)
Ca-O(9b)	2.597(5)	Ca(2d)-O(3b)	2.355(5)	Mg-O(6d)	2.067(5)	Si(1)-O(1d)	1.625(5)
Ca-O(9b)	2.594(5)	Ca(2d)-O(4d)	2.454(5)	Mg-O(10)	2.023(6)		
		Ca(2d)-O(5c)	2.345(5)			Si(2a)-O(2c)	1.655(5)
Ca(1a)-O(1a)	2.355(5)	Ca(2d)-O(5d)	2.439(5)	Al(1a)-O(4c)	1.943(5) [×2]	Si(2a)-O(3c)	1.645(5)
Ca(1a)-O(1a)	2.355(5)	Ca(2d)-O(6b)	2.959(5)	Al(1a)-O(8a)	1.881(4) [×2]	Si(2a)-O(4c)	1.666(5)
Ca(1a)-O(1b)	2.345(5)	Ca(2d)-O(8b)	2.335(5)	Al(1a)-O(11a)	1.882(5) [×2]	Si(2a)-O(7c)	1.613(5)
Ca(1a)-O(1b)	2.345(5)						
Ca(1a)-O(2a)	2.527(5)	Ca(3a)-O(3a)	2.446(5)	Al(1b)-O(4d)	1.951(5) [×2]	Si(2b)-O(2d)	1.647(5)
Ca(1a)-O(2a)	2.527(5)	Ca(3a)-O(6a)	2.485(5)	Al(1b)-O(8b)	1.875(4) [×2]	Si(2b)-O(3d)	1.643(5)
Ca(1a)-O(2b)	2.518(5)	Ca(3a)-O(6c)	2.979(5)	Al(1b)-O(11b)	1.875(5) [×2]	Si(2b)-O(4d)	1.672(5)
Ca(1a)-O(2b)	2.518(5)	Ca(3a)-O(7a)	2.575(5)			Si(2b)-O(7d)	1.612(5)
		Ca(3a)-O(7b)	2.511(5)	Al(1c)-O(4a)	1.933(5) [×2]		
Ca(1b)-O(1c)	2.355(4)	Ca(3a)-O(7c)	2.401(5)	Al(1c)-O(8c)	1.886(4) [×2]	Si(2c)-O(2a)	1.647(5)
Ca(1b)-O(1c)	2.355(4)	Ca(3a)-O(8a)	2.613(5)	Al(1c)-O(11c)	1.878(4) [×2]	Si(2c)-O(3b)	1.643(5)
Ca(1b)-O(1d)	2.350(4)	Ca(3a)-O(10)	2.560(6)			Si(2c)-O(4a)	1.685(5)
Ca(1b)-O(1d)	2.350(4)	Ca(3a)-O(11a)	2.503(5)	Al(1d)-O(4b)	1.932(5) [×2]	Si(2c)-O(7a)	1.620(5)
Ca(1b)-O(2c)	2.515(5)			Al(1d)-O(8d)	1.879(4) [×2]		
Ca(1b)-O(2c)	2.516(5)	Ca(3b)-O(3b)	2.442(5)	Al(1d)-O(11d)	1.877(5) [×2]	Si(2d)-O(2b)	1.642(5)
Ca(1b)-O(2d)	2.525(5)	Ca(3b)-O(6b)	2.482(5)			Si(2d)-O(3a)	1.651(5)
Ca(1b)-O(2d)	2.525(5)	Ca(3b)-O(6d)	2.988(5)	Al(2a)-O(1a)	1.943(5)	Si(2d)-O(4b)	1.685(5)
		Ca(3b)-O(7a)	2.505(5)	Al(2a)-O(2a)	1.907(5)	Si(2d)-O(7b)	1.616(5)
Ca(2a)-O(1a)	2.485(5)	Ca(3b)-O(7b)	2.572(5)	Al(2a)-O(3a)	1.979(5)		
Ca(2a)-O(2a)	2.441(5)	Ca(3b)-O(7d)	2.400(5)	Al(2a)-O(4c)	2.093(5)	Si(3a)-O(5c)	1.635(5)
Ca(2a)-O(3c)	2.365(5)	Ca(3b)-O(8b)	2.614(5)	Al(2a)-O(5a)	2.017(5)	Si(3a)-O(6b)	1.619(5)
Ca(2a)-O(4a)	2.455(5)	Ca(3b)-O(10)	2.570(5)	Al(2a)-O(11a)	1.930(5)	Si(3a)-O(8c)	1.622(5)
Ca(2a)-O(5a)	2.432(5)	Ca(3b)-O(11b)	2.497(5)			Si(3a)-O(9a)	1.656(5)
Ca(2a)-O(5a)	2.349(5)			Al(2b)-O(1b)	1.957(5)		
Ca(2a)-O(6c)	2.965(5)	Ca(3c)-O(3c)	2.443(5)	Al(2b)-O(2b)	1.922(5)	Si(3b)-O(5d)	1.629(5)
Ca(2a)-O(8c)	2.333(4)	Ca(3c)-O(6b)	2.988(5)	Al(2b)-O(3b)	1.983(5)	Si(3b)-O(6a)	1.613(5)
		Ca(3c)-O(6c)	2.477(5)	Al(2b)-O(4d)	2.092(5)	Si(3b)-O(8d)	1.629(5)
Ca(2b)-O(1b)	2.479(5)	Ca(3c)-O(7a)	2.401(5)	Al(2b)-O(5b)	2.021(5)	Si(3b)-O(9b)	1.662(5)
Ca(2b)-O(2b)	2.436(5)	Ca(3c)-O(7c)	2.504(5)	Al(2b)-O(11b)	1.951(5)		
Ca(2b)-O(3d)	2.363(5)	Ca(3c)-O(7c)	2.580(5)			Si(3c)-O(5a)	1.632(5)
Ca(2b)-O(4b)	2.471(5)	Ca(3c)-O(8c)	2.620(5)	Al(2c)-O(1c)	1.949(5)	Si(3c)-O(6c)	1.615(5)
Ca(2b)-O(5b)	2.426(5)	Ca(3c)-O(10)	2.562(7)	Al(2c)-O(2c)	1.916(5)	Si(3c)-O(8a)	1.636(5)
Ca(2b)-O(5b)	2.341(5)	Ca(3c)-O(11c)	2.499(5)	Al(2c)-O(3c)	1.975(5)	Si(3c)-O(9a)	1.661(5)
Ca(2b)-O(6d)	2.967(5)			Al(2c)-O(4a)	2.082(5)		
Ca(2b)-O(8d)	2.335(5)	Ca(3d)-O(3d)	2.447(5)	Al(2c)-O(5c)	2.022(5)	Si(3d)-O(5b)	1.637(5)
		Ca(3d)-O(6a)	2.983(5)	Al(2c)-O(11c)	1.939(5)	Si(3d)-O(6d)	1.617(5)
Ca(2c)-O(1d)	2.486(5)	Ca(3d)-O(6d)	2.483(5)			Si(3d)-O(8b)	1.632(5)
Ca(2c)-O(2c)	2.441(5)	Ca(3d)-O(7b)	2.396(5)	Al(2d)-O(1d)	1.946(5)	Si(3d)-O(9b)	1.667(5)
Ca(2c)-O(3a)	2.360(5)	Ca(3d)-O(7d)	2.511(5)	Al(2d)-O(2d)	1.917(5)		
Ca(2c)-O(4c)	2.466(5)	Ca(3d)-O(7d)	2.577(5)	Al(2d)-O(3d)	1.977(5)		
Ca(2c)-O(5c)	2.426(5)	Ca(3d)-O(8d)	2.616(5)	Al(2d)-O(4b)	2.081(5)		

vesuvianite. However, the OH^- dipole is randomly oriented in the present vesuvianite. Therefore, it is suggested that the low symmetry of the specimen is not due to preferred orientation of OH^- dipoles.

Akizuki (1981) proposed a formation mechanism for cation ordering in zeolites and some other minerals. Since the atomic ordering occurs by a charge balance of atoms along growth steps, if the growth steps are normal to the

Table 6*b*. Selected interatomic distances (Å) of the {111} sector.

Ca-O(6a)	2.294(9)	Ca(2c)-O(5c)	2.427(8)	Ca(3d)-O(7d)	2.608(8)	Al(2d)-O(3d)	1.990(8)
Ca-O(6b)	2.292(9)	Ca(2c)-O(5d)	2.341(8)	Ca(3d)-O(8d)	2.606(8)	Al(2d)-O(4b)	2.089(8)
Ca-O(6c)	2.28(1)	Ca(2c)-O(6a)	2.979(8)	Ca(3d)-O(10)	2.58(1)	Al(2d)-O(5d)	2.026(8)
Ca-O(6d)	2.30(1)	Ca(2c)-O(8a)	2.324(8)	Ca(3d)-O(11d)	2.503(8)	Al(2d)-O(11d)	1.933(9)
Ca-O(9a)	2.608(9)						
Ca-O(9a)	2.602(9)	Ca(2d)-O(1c)	2.472(8)	Mg-O(6a)	2.062(8)	Si(1)-O(1a)	1.634(8)
Ca-O(9b)	2.618(9)	Ca(2d)-O(2d)	2.437(8)	Mg-O(6b)	2.064(9)	Si(1)-O(1b)	1.634(8)
Ca-O(9b)	2.621(9)	Ca(2d)-O(3b)	2.372(7)	Mg-O(6c)	2.053(9)	Si(1)-O(1c)	1.637(8)
		Ca(2d)-O(4d)	2.463(8)	Mg-O(6d)	2.071(9)	Si(1)-O(1d)	1.624(8)
Ca(1a)-O(1a)	2.335(8)	Ca(2d)-O(5c)	2.354(8)	Mg-O(10)	2.071(9)		
Ca(1a)-O(1a)	2.334(8)	Ca(2d)-O(5d)	2.437(8)			Si(2a)-O(2c)	1.651(8)
Ca(1a)-O(1b)	2.350(7)	Ca(2d)-O(6b)	2.961(8)	Al(1a)-O(4c)	1.943(7) [×2]	Si(2a)-O(3c)	1.639(8)
Ca(1a)-O(1b)	2.350(7)	Ca(2d)-O(8b)	2.333(8)	Al(1a)-O(8a)	1.894(8) [×2]	Si(2a)-O(4c)	1.671(8)
Ca(1a)-O(2a)	2.510(8)			Al(1a)-O(11a)	1.867(8) [×2]	Si(2a)-O(7c)	1.609(8)
Ca(1a)-O(2a)	2.511(8)	Ca(3a)-O(3a)	2.422(8)				
Ca(1a)-O(2b)	2.530(8)	Ca(3a)-O(6a)	2.504(8)	Al(1b)-O(4d)	1.943(7) [×2]	Si(2b)-O(2d)	1.643(8)
Ca(1a)-O(2b)	2.529(8)	Ca(3a)-O(6c)	3.000(8)	Al(1b)-O(8b)	1.885(8) [×2]	Si(2b)-O(3d)	1.635(8)
		Ca(3a)-O(7a)	2.610(8)	Al(1b)-O(11b)	1.864(7) [×2]	Si(2b)-O(4d)	1.668(8)
Ca(1b)-O(1c)	2.343(7)	Ca(3a)-O(7b)	2.506(8)	Al(1c)-O(4a)	1.947(7) [×2]	Si(2b)-O(7d)	1.617(8)
Ca(1b)-O(1c)	2.343(7)	Ca(3a)-O(7c)	2.382(8)	Al(1c)-O(8c)	1.893(8) [×2]		
Ca(1b)-O(1d)	2.344(7)	Ca(3a)-O(8a)	2.610(8)	Al(1c)-O(11c)	1.844(7) [×2]	Si(2c)-O(2a)	1.643(8)
Ca(1b)-O(1d)	2.344(7)	Ca(3a)-O(10)	2.571(9)			Si(2c)-O(3b)	1.644(8)
Ca(1b)-O(2c)	2.514(9)	Ca(3a)-O(11a)	2.497(8)	Al(1d)-O(4b)	1.951(8) [×2]	Si(2c)-O(4a)	1.667(8)
Ca(1b)-O(2c)	2.513(9)			Al(1d)-O(8d)	1.880(8) [×2]	Si(2c)-O(7a)	1.605(8)
Ca(1b)-O(2d)	2.519(8)	Ca(3b)-O(3b)	2.442(8)	Al(1d)-O(11d)	1.859(7) [×2]		
Ca(1b)-O(2d)	2.519(8)	Ca(3b)-O(6b)	2.491(8)			Si(2d)-O(2b)	1.660(8)
		Ca(3b)-O(6d)	2.988(8)	Al(2a)-O(1a)	1.956(8)	Si(2d)-O(3a)	1.634(8)
Ca(2a)-O(1a)	2.464(8)	Ca(3b)-O(7a)	2.491(9)	Al(2a)-O(2a)	1.920(8)	Si(2d)-O(4b)	1.665(8)
Ca(2a)-O(2a)	2.437(8)	Ca(3b)-O(7b)	2.599(8)	Al(2a)-O(3a)	1.992(8)	Si(2d)-O(7b)	1.603(8)
Ca(2a)-O(3c)	2.377(8)	Ca(3b)-O(7d)	2.373(8)	Al(2a)-O(4c)	2.096(8)		
Ca(2a)-O(4a)	2.455(7)	Ca(3b)-O(8b)	2.624(8)	Al(2a)-O(5a)	2.025(9)	Si(3a)-O(5c)	1.631(8)
Ca(2a)-O(5a)	2.423(8)	Ca(3b)-O(10)	2.57(1)	Al(2a)-O(11a)	1.936(8)	Si(3a)-O(6b)	1.616(8)
Ca(2a)-O(5a)	2.341(8)	Ca(3b)-O(11b)	2.501(8)			Si(3a)-O(8c)	1.630(8)
Ca(2a)-O(6c)	2.963(9)			Al(2b)-O(1b)	1.952(8)	Si(3a)-O(9a)	1.656(9)
Ca(2a)-O(8c)	2.317(8)	Ca(3c)-O(3c)	2.424(8)	Al(2b)-O(2b)	1.899(8)		
		Ca(3c)-O(6b)	2.987(8)	Al(2b)-O(3b)	1.973(8)	Si(3b)-O(5d)	1.625(8)
Ca(2b)-O(1b)	2.466(8)	Ca(3c)-O(6c)	2.480(8)	Al(2b)-O(4d)	2.094(8)	Si(3b)-O(6a)	1.607(8)
Ca(2b)-O(2b)	2.441(8)	Ca(3c)-O(7a)	2.394(8)	Al(2b)-O(5b)	2.013(9)	Si(3b)-O(8d)	1.619(8)
Ca(2b)-O(3d)	2.364(8)	Ca(3c)-O(7c)	2.494(8)	Al(2b)-O(11b)	1.935(8)	Si(3b)-O(9b)	1.653(8)
Ca(2b)-O(4b)	2.449(8)	Ca(3c)-O(7c)	2.606(8)				
Ca(2b)-O(5b)	2.433(8)	Ca(3c)-O(8c)	2.612(8)	Al(2c)-O(1c)	1.952(8)	Si(3c)-O(5a)	1.632(8)
Ca(2b)-O(5b)	2.355(8)	Ca(3c)-O(10)	2.57(1)	Al(2c)-O(2c)	1.913(8)	Si(3c)-O(6c)	1.627(8)
Ca(2b)-O(6d)	2.967(9)	Ca(3c)-O(11c)	2.509(8)	Al(2c)-O(3c)	1.977(8)	Si(3c)-O(8a)	1.620(8)
Ca(2b)-O(8d)	2.338(7)			Al(2c)-O(4a)	2.092(8)	Si(3c)-O(9a)	1.662(9)
		Ca(3d)-O(3d)	2.439(8)	Al(2c)-O(5c)	2.019(8)		
Ca(2c)-O(1d)	2.475(8)	Ca(3d)-O(6a)	2.980(8)	Al(2c)-O(11c)	1.929(9)	Si(3d)-O(5b)	1.636(8)
Ca(2c)-O(2c)	2.445(8)	Ca(3d)-O(6d)	2.499(9)			Si(3d)-O(6d)	1.601(8)
Ca(2c)-O(3a)	2.370(8)	Ca(3d)-O(7b)	2.385(8)	Al(2d)-O(1d)	1.962(8)	Si(3d)-O(8b)	1.610(8)
Ca(2c)-O(4c)	2.452(8)	Ca(3d)-O(7d)	2.503(8)	Al(2d)-O(2d)	1.928(8)	Si(3d)-O(9b)	1.670(9)

symmetrical mirror plane, the mirror plane will be maintained during growth. If the steps are inclined to the mirror plane, the structure will not have the symmetry of the morphological symmetry plane.

The crystal structure of vesuvianite is similar to that of grandite garnet, and Akizuki (1984) suggested that the low-symmetry sector of grandite garnet is produced by same mechanism

TABLE 7. Al/Fe occupancies of the {110} and {111} sectors in vesuvianite.

{110} sector			
Al(1a)	$Al_{0.483(3)}Fe_{0.017}$	Al(2a)	$Al_{0.780(5)}Fe_{0.220}$
Al(1b)	$Al_{0.479(3)}Fe_{0.021}$	Al(2b)	$Al_{0.809(5)}Fe_{0.191}$
Al(1c)	$Al_{0.474(3)}Fe_{0.026}$	Al(2c)	$Al_{0.798(5)}Fe_{0.202}$
Al(1d)	$Al_{0.473(3)}Fe_{0.027}$	Al(2d)	$Al_{0.820(5)}Fe_{0.180}$
{111} sector			
Al(1a)	$Al_{0.484(5)}Fe_{0.016}$	Al(2a)	$Al_{0.801(7)}Fe_{0.199}$
Al(1b)	$Al_{0.487(5)}Fe_{0.013}$	Al(2b)	$Al_{0.738(7)}Fe_{0.262}$
Al(1c)	$Al_{0.478(5)}Fe_{0.022}$	Al(2c)	$Al_{0.706(7)}Fe_{0.294}$
Al(1d)	$Al_{0.486(5)}Fe_{0.014}$	Al(2d)	$Al_{0.743(7)}Fe_{0.257}$

The population of Fe was calculated by the difference between full population and calculated population of Al.

proposed by Akizuki (1981). Thus, the symmetry of monoclinic vesuvianite with sectors can be explained by this mechanism. The (110) and (111) faces of vesuvianite are inclined to the (001) and (100) morphological symmetry planes, resulting in the ordered structure with respect to the Al and Fe atoms. Allen and Burnham (1992) suggested this was the origin of the optical anomaly of vesuvianite as well, because the texture is similar to that of zeolites (e.g. Akizuki, 1981).

The monoclinic ordered structure is stable rather than the tetragonal disordered one at low temperature, because the tetragonal structure transforms to monoclinic in nature (Veblen and Wiechmann, 1991). The vesuvianite we have studied, which consists of both stable and metastable phases, was produced during non-equilibrium growth.

Acknowledgements

We are grateful to T. Ohyama and Y. Ito for their assistance.

References

Akizuki, M. (1981) Origin of optical variation in analcime. *American Mineralogist*, **66**, 403–9.

Akizuki, M. (1984) Origin of optical variation in grossular-andradite garnet. *American Mineralogist*, **69**, 328–38.

Akizuki, M. and Sunagawa, I. (1978) Study of the sector structure in adularia by means of optical microscopy, infra-red absorption, and electron microscopy. *Mineralogical Magazine*, **42**, 453–62.

Akizuki, M. and Terada, T. (1998) Origin of abnormal property of apophyllite. *Neues Jahrbuch für Mineralogie, Monatshefte*, 234–40.

Akizuki, M., Hampar, M. and Zussman, J. (1979) An explanation of anomalous optical properties of topaz. *Mineralogical Magazine*, **43**, 237–41.

Allen, F. and Burnham, C. (1992) A comprehensive structure-model for vesuvianite: symmetry variation and crystal growth. *The Canadian Mineralogist*, **30**, 1–18.

Armbruster, T. and Gnos, E. (2000) *P4/n* and *P4nc* long-range ordering in low-temperature vesuvianites. *American Mineralogist*, **85**, 563–9.

Brauns, R. (1883) Ueber die Ursache der anomalen Doppelbrechung einiger regulär krystallisirender Salze. *Neues Jahrbuch für Mineralogie, Geologie und Palaeontologie*, 102–11.

Brauns, R. (1891) *Die Optischen Anomalien der Krystalle*. S. Hirzel, Leipzig, Germany.

Fitzgerald, S., Rheingold, A. and Leavens, P. (1986) Crystal stucture of a non-*P4/nnc* vesuvianite from Asbestos, Quebec. *American Mineralogist*, **71**, 1483–8.

Fitzgerald, S., Leavens, P., Rheingold, A. and Nelen, J. (1987) Crystal structure of a *REE*-bearing vesuvianite from San Benito County, California. *American Mineralogist*, **72**, 625–8

Groat, L., Hawthorne, F. and Ercit, T. (1992) The chemistry of vesuvianite. *The Canadian Mineralogist*, **30**, 19–48.

Groat, L., Hawthorne, F., Ercit, T. and Putnis, A. (1993) The symmetry of vesuvianite. *The Canadian Mineralogist*, **31**, 617–35.

Groat, L., Hawthorne, F., Rossman, G. and Ercit, T. (1995) The infrared spectroscopy of vesuvianite in the OH region. *The Canadian Mineralogist*, **33**, 609–26.

International Tables for X-ray Crystallography (1974)

The Kynoch Press, Birmingham, England.

Johnson, T.E., Hudson, N.F.C. and Droop, G.T.R. (2000) Wollastonite-bearing assemblages from the Dalradian at Fraserburgh, northeast Scotland and their bearing on the emplacement of garnetiferous granitoid sheets. *Mineralogical Magazine*, **64**, 1165–1176.

Lager, G., Xie, Q., Ross, F., Rossman, G., Armbruster, T., Rotella, F. and Schultz, A. (1999) Hydrogen-atom positions in *P4/nnc* vesuvianite. *The Canadian Mineralogist*, **37**, 763–8.

Mallard, E. (1877) Ueber anomale optische Erscheinungen an Krystallen. *Zeitschrift für Kristallographie und Mineralogie*, 309–20.

Matsubara, S., Miyawaki, R., Kato, A., Yokoyama, K. and Okamoto, A. (1998) Okayamalite, $Ca_2B_2SiO_7$, a new mineral, boron analogue of gehlenite. *Mineralogical Magazine*, **62**, 703-706

Molecular Structure Corporation (1985, 1992) *teXsan: Crystal structure analysis package*. Molecular Structure Corporation, Texas, USA.

Ohkawa, M., Yoshiasa, A. and Takeno, S. (1994) Structural investigation of high- and low-symmetry vesuvianite. *Mineralogical Journal*, **17**, 1–20.

Shtukenberg, A.G., Punin, Yu.O. and Soloviev, V.N. (2000) Effect of growth conditions on the birefringence of mixed crystals revealed in alum solid solutions. *Mineralogical Magazine*, **64**, 837–45.

Shtukenberg, A.G., Punin, Yu.O., Frank-Kamenetskaya, O.V., Kovalev, O.G. and Sokolov, P.B. (2001) On the origin of anomalous birefringence in grandite garnets. *Mineralogical Magazine*, **65**, 445–59.

Veblen, D. and Wiechmann, M. (1991) Domain structure of low-symmetry vesuvianite from Crestmore, California. *American Mineralogist*, **76**, 397–404.

Warren, B. and Modell, D. (1931) The structure of vesuvianite $Ca_{10}Al_4(Mg, Fe)_2Si_9O_{34}(OH)_4$. *Zeitschrift für Kristallographie*, **78**, 422–32.

[*Manuscript received 22 March 2001: revised 23 January 2002*]